Global Scientific and Academic Research Journal of Multidisciplinary Studies
ISSN: 2583-4088 (Online)
Frequency: Monthly
Published By GSAR Publishers
Journal Homepage Link- https://gsarpublishers.com/journals-gsarjms-home/

Enhanced Dielectric and Piezoelectric Properties of $BaTiO_3$-Infused $K_{0.3}Na_{0.2}Bi_{0.5}TiO_3$ Ceramics for High-Frequency Applications

By

Muhammad Nasir Rafiq[1], Maryam Liaqat[2], Maleha Sadiqa[3], Hamza Shams[4], Muhammad Farrukh[5], Rubab Sarfraz[6], Maneeb Ur Rehman[7], Waheed Zaman Khan[8]

[1]Department of Opto-Electronics, Xi'an Technological University, China
[2]College of Electronics and Information Engineering, Shenzhen University, Shenzhen 518060, China
[3]Department of Chemistry, Govt. College University Faisalabad, Faisalabad, 38000, Punjab, Pakistan
[4]Department of Physics, University of Peshawar, Khyber Pakhtunkhwa 25120, Pakistan
[5]Department of Chemical, Polymer and Composite Materials Engineering UET Lahore, Punjab 54890, Pakistan
[6]Department of Chemistry, University of Agriculture Faisalabad, Punjab, Pakistan
[7]Department of Physics, Faculty of Basic and Applied Sciences (FBAS), International Islamic University (IIU), H-10, Islamabad, 44000, Pakistan
[8]Department of Physics, Division of Science and Technology, University of Education, Lahore, Punjab 54770, Pakistan.

Article History

Received: 15/02/2025
Accepted: 26/02/2025
Published: 28/02/2025

Vol – 4 Issue –2

PP: - 94-100

DOI:10.5281/zenodo.14956707

Abstract

In the present study, $BaTiO_3$-modified $K_{0.3}\ Na_{0.2}\ Bi_{0.5}TiO_3$ (KNNBT) ceramics were prepared using a solid-state reaction method. The influence of $BaTiO_3$ (BT) addition on the microstructure, dielectric, ferroelectric, and piezoelectric properties of KNNBT ceramics was investigated. The study's finding shows that the dielectric properties of BT-modified KNT ceramics were significantly improved compared to those of pure KNT ceramics. The maximum dielectric constant was about 21000 for the BT-modified KNT ceramic with a BT content of 0.1 mol %. The addition of BT significantly enhanced the densification of KNT ceramics. The enhanced densification was ascribed to the forming of a BT-rich phase, which acted as a nucleating agent. The BaTiO3-modified KNNBT ceramics showed a good piezoelectric response with the piezoelectric coefficient d33 of 451 PC/N. The results suggest that the BT-modified KNT ceramics are promising candidates for high-frequency applications.

Keywords: *BT (barium titanate/ $BaTiO_3$), Dielectric, Piezoelectric KNT (Potassium Sodium titanate), Solid-State Reaction.*

Introduction

The development of microwave telecommunication technology has led to the rapid growth of microwave communications & information systems during the previous few years. Increasing the number of customers and rapid growth of mobile cell phone-making industries are common examples of its large-scale applications[1]. The revolution in this field results from endless exploration of material science, particularly in dielectric ceramics. Dielectric ceramics with specific compositions of different dopants make them suitable for microwave devices or dielectric resonator applications at the range of microwave frequencies. Low dielectric loss and high dielectric constant ceramic material can lead to electronic equipment's miniaturization. The simple and complex perovskite ceramics are based on titanate and niobate and are used as dielectric resonators in mobile phones, handsets, and base station applications[2].In the early 1990s, the rapid rise of the mobile phone market prompted extensive study into producing low-cost, advanced-architecture materials. Combining two ABO_3 systems with appropriate stoichiometry can enhance the various properties of materials. Composites are the best examples, and composite material has been designed to modify the microwave dielectric properties compared to individual properties. A few composite samples arrived, which might result from the mutual communication between the elements. Mathematical intentions could give an ideal geometrical shape of the composite that may affect phase & microstructural properties. Still, the chemistry in composite processing restricts the elements' geometry. Processing route and their parameters play a key role in the growth of geometry & microstructure of ceramic composite.

*Corresponding Author: **Muhammad Nasir Rafiq**

These composites were characterized in three ways, i.e., Bulk, macro, &Nano structures[2]. Barium titanate, developed between the 1940s & 1950s, was the first oxide with a perovskite-type structure showing dielectric behavior [3-5]. It has a relatively large electromechanical coupling factor (k33) (Stored mechanical energy/Input electrical energy) and takings for dielectric applications such as resonators while its chief usage for dielectric applications owing to its very high relative permittivity [6-8]. Barium Titanate ($BaTiO_3$) is the classic ferroelectric perovskite material. Its cubic perovskite-type and three-dimensional networks of corner-sharing octahedral of O_2-ions. At higher temperatures, it is cubic (Para electric), but on cooling, it becomes tetragonal (ferroelectric) below Curie temperature of 410 K, orthorhombic below 290 K, and rhombohedral below 190 K [9, 10]. The electrical performance of perovskite ceramics can be improved by doping at the A-site and B-site. Many research studies have been done on the iso-valent/off-valent substitution in BT systems [11].The substitution of crystal atoms by another iso valent cation, such as Ba, Mg, Ca, and Sr, modifies the dielectric properties and transition temperature and shows diffuse phase transition [12].Additionally, we obtained the desired thermal stability in the dielectric properties of the BT system. Doping with A-site cations of the same valence and comparable ionic radius as Ba affects the Curie temperature Tc (~120 ℃ in $BaTiO_3$) to either decreases in (Sr substitution) or increases in (Ca substitutions) without any significant broadening of phase transitions (R) [13-15]. The addition of Ca^{2+} to the site A of $BaTiO_3$ increases the stability temperature range of the tetragonal phase by shifting to lower values of the ferroelectric – rhombohedral to orthorhombic and orthorhombic to tetragonal phase transition [16, 17]. Bismuth potassium titanate ($Bi_{0.5}K_{0.5}$) TiO_3 (BKT) is a good Ferro as well as a dielectric material that has a tetragonal structure at room temperature and possesses a high curie temperature of about 380℃ [18]. Ivanova researcher investigated the structure of BKT dielectric ceramics using XRD analysis and revealed that the lattice parameters of BKT ceramics are a = 0.391 nm, c = 0.399 nm. They also revealed that second-phase formation with a transition temperature of about 170℃. The Curie temperature (Tc) of ($Bi_{0.5}K_{0.5}$) TiO_3, which belongs to the same series as bismuth alkali titanate, is 320 C. However, BNT has a T_C of about 200 ^oC, the same as that of BKT. The phase boundary between the rhombohedra ferroelectric and antiferroelectric phase fields and piezoelectricity disappear at T_C. BKT ceramics seem to be a candidate for lead-free piezoelectric with a high T_C. Nevertheless, for the same reason for BNT, it is necessary to clarify the electrical behavior at T_C. Although the electrical properties of some BKT-based ceramics have been reported by many researchers [19-21]. Some researchers have reported studies on BKT ceramics and their electrical properties because it is difficult to prepare a dense ceramic body using a conventional ceramic fabrication process. $Bi_{0.5}(Na_{1-x}K_x)_{0.5}TiO_3$ ceramics exhibit morphotropic phase boundary (MPB) separating rhombohedral BNT and tetragonal BKT structures in the range of x = 0.16–0.20 [22]. Dielectric and piezoelectric properties of BNKT ceramics are enhanced near the MPB region. The maximum dielectric constant (ε_r = 1030) and piezoelectric coefficient (d33 = 151 pC/N) were obtained at x = 0.20. $BaTiO_3$ (BT) is an inorganic compound with a perovskite structure and possesses typical dielectric, ferroelectric, piezoelectric, and insulating properties. This material exhibits a high dielectric constant at room temperature [23].It is reported that a phase transition from the coexistence of ferroelectric tetragonal and rhombohedra to a relaxer pseudo cubic with a significant disruption of the long-range ferroelectric order in modified strontium zirconate composite [24].In this work, we will check the Dielectric and piezoelectric properties of BaTiO3 modified-KNT by using the solid-state reaction method.

Experimental Methods

There are many methods or routes for synthesizing various types of ceramics material. We have used only a mixed oxide route to synthesize BaTiO3-doped KNaBiTiO3 ceramics.

Mixed oxide route

The preparation of ceramic products typically includes heating methods of ceramic powders, which ought to go through special handling to handle purity, length of particles, size distribution of particles, and diversity [25]. The solid-state reaction, metal oxide, or ceramic methods are low-priced and mainly used for manufacturing MW dielectric ceramic materials in various industries.

Figure.1 Step by step process of metal oxide route.

The mixed oxide route is frequently applied to manufacture complex oxide from simple oxides, nitrates, carbonates, hydroxides, alko-oxides, oxalates, etc. Typically, the process involves various heating steps of the powder with many intermediary grinding steps to increase the mixture's consistency and minimize the size of the particles. The initial reactants should have a large surface area to increase the contact between reactants. Additional milling or grinding makes the powder more effective in later annealing treatment measures (i.e., more active sinter). A mixed oxide route is less expensive and requires simpler things. Therefore, a large amount of powder can be prepared [26]. Complete milling is required to attain the reactants of a homogenous mixture. The number of crystallites in contact can be enhanced by pelletizing the powders using a hydraulic press. Each material possesses small crystallites, so the powder sample is pelletized to enable good contact with typical micrometer-sized particles. The reaction mixture is generally removed and reintroduced to bring fresh surfaces in touch, speeding up the process. Intermediate milling can sometimes take hours but a few days or weeks for a complete response.

The ceramic powder is then treated thermally, known as calcination. Over an average time scale, solids do not react at room temperature. Hence, they must be calcinated at 1000-

*Corresponding Author: **Muhammad Nasir Rafiq**

1500°C temperatures to provide the reaction's thermodynamics and kinetics. Thermodynamics and kinetics factors of the response are essential because they decide whether the reaction should occur and determine the reaction's rate, respectively. After the calcination re-milling process, the powder is passed through a manual press instrument, creating pallets of 10.0mm in diameter and 3.0 to 5.0mm in height, with a pressure of 7 tons/in^2. During the powder press process to form ceramics, heat, and pressure are used to densify and bind ceramics together, which is called sintering.

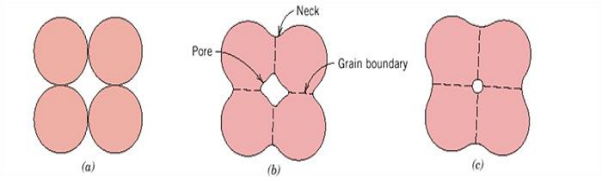

Figure. 1 During powder press processes, Pressure heat binds and densifies ceramics together.

Ceramic materials tend to have high melting temperatures, so the process of sintering (done at temperatures below bulk melting temperatures) provides remarkable energy savings. Powder X-ray diffraction is usually used to test sample purity. Resistance heating with metal, SiC, or $MoSi_2$ heating components is used in the furnaces. A CO_2 laser can deliver temperatures of up to 4300 K. In converting electrical energy into heat energy (up to 2200 K), an Electric arc directed at the sample can receive 3300 K. Crucible (containers for the reaction) need to resist high temperatures and be relatively inert to the reactants. Ordinary crucibles are alumina (to 2200 K), silica (to 1430 K), zirconia (to 2300 K), or magnesia (to 2700 K). Silver (m.p. 1235 K) and Platinum (m.p. 2045 K) can also be used for reactions.

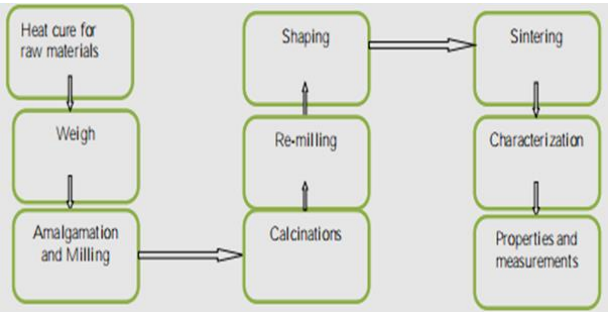

Figure 3: The metal oxide route block diagram.

Raw Materials

The enlisted raw materials were used in the processing of the products.

Table 1 Raw materials used in the processing of products

S. No	Chemicals	Formula	Foundation	Purity (%)	Calcination (°C)
	Barium Carbonate	$BaCO_3$	Aldrich	99.0	800
	Titanium Oxide	TiO_2	Sigma,	99.9	800
	Bismuth Oxide	Bi_2O_3	Sigma	99.6	800
	Sodium Carbonate	Na_2CO_3	Aldrich	99.5	800
	Potassium Carbonate	K_2CO_3	Aldrich	99.5	800

After selecting the required reactant materials with proposed ratios, they are mixed and ground using horizontal ball milling to make proper compositions for each sample. Ball milling machines are generally very slow but much easier to use. Milling has been shown to impact a material's microwave dielectric characteristics significantly. [27-29]. We treated the material with heat from 200°C to 800°C for three hours before measuring to remove moisture and hydroxide.

XRD (X-ray Diffraction)

X-ray diffraction (XRD) is one of the characterizing techniques, which is nondestructive and reveals information about the stress measurement, crystallographic structure, study of phase equilibrium, physical composition of materials, chemical composition, plane orientations, and crystallite size of the crystal. The monochromatic X-ray is produced in a glass tube with gases at low pressure. The x-ray interaction with mater (sample) created many phenomena, obeys interference rules & satisfies Braggs law as well as shown in Figure 4.

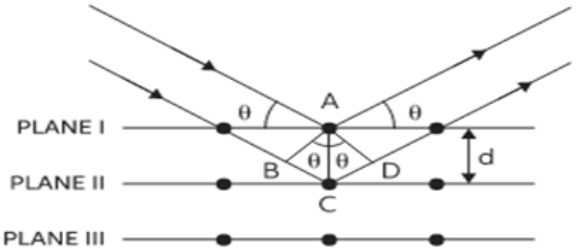

Figure. 4 X-ray diffraction patterns on the atomic plane.

In this study, the X-ray powder-diffractogram of all the studies samples was recorded along with Rigaku Mini fix-diffractometer (Japan) using Cu-K_α (λ = 1.5418Å) radiations with Ni-filter in wide Braggs angle (2θ) range by scanning rate of 3°/min at material research laboratory (MRL),

University of Peshawar, Pakistan. The tube's operating source voltage & current are 30kV and 10mA, respectively. X-Ray radiation may be diverted up to 3° to 5° in the vertical (y-axis) direction.[4, 30]The sample profile intensity distribution data will be recorded accurately after setting and adjusting the XRD machine with silicon standards.

Calculation of particle size

Many properties of solid materials are strongly dependent on the crystallite size. The properties like density, porosity, elastic modulus in mechanics, resistivity and magnetization in electricity and magnetism, and the dielectric constant in optics were strongly affected by particle size. The properties like microwave dielectric can drastically change when nanometer measurements are made. Scherer formula (Patterson 1939) can be used to find the crystallite size from XRD patterns.

$$D = \frac{0.9\lambda}{\beta\cos\theta} \quad \text{(a)}$$

Where ‘β’ does the equation calculate the total width half maximum (FWHM)?

$$\beta = \sqrt{\beta_M^2 - \beta_S^2} \quad \text{(b)}$$

Where the diameter is ‘D’ of particles, the X-ray wavelength is ‘λ’ (0.154 nm), The broadening peak measurement is ‘βM,’ and the instrumental broadening peak is ‘β_S’ in radian and ‘θ’ is Bragg angle for reflection.

FTIR (Fourier transform infrared radiation) spectroscopy

The FTIR approach evaluates material accessible in limited quantities or as a single entity. FTIR Microscope usually analyses a sample contaminated with inorganic components; usually, a sample size of ~20 Microns can also be analyzed. It is often used for qualitative identifications of diverse capabilities, but quantitative analysis must be used with well-defined standards. The components of radiations are not physically separated in FTIR Spectroscopy equipment; instead, the radiations were evaluated inside the time-dependent frame of reference (the time area) by passing through the Michelson Interferometer. In this interferometer, light is separated into two beams by a beam splitter, and another beam strikes a moving mirror, which is reflected to the beam splitter. The beam proceeds on the sample and the detector after recombining two beams at the beam splitter[31]. After combining the two beams, the difference in path length of the two beams, which is an integral wavelength multiple, will determine whether they interfere destructively or constructively. The retardation is the difference in path length; therefore, the interference is maximally constructive.

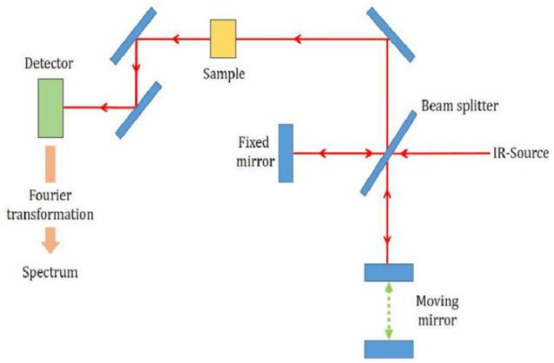

Figure 5: Schematic illustration of an FTIR spectrometer.

SEM (Scanning electron microscopy)

In 1938, Siemens used SEM’ practically and marketed it in 1965. 1965 Cambridge Scientific Instruments launched the first commercial SEM for bulk samples. Its resolution at that time was ~50 nm; today, it is less than 1nm. [32]. It was initially used to study the morphology of the samples, whereas now it is more of an analytical instrument. The essential features of SEM include composition, morphology (shape and size of the particles making up the object), topography, and crystallographic information (how the atoms are arranged). The typical accelerating potential used for SEM is 0-30 kV [33]. The sample surface has been coated for microstructural (SEM) characterizations of all samples, which are to be coated by sputtering. Still, gold, and thus, the sample is made highly polished and conductive. The gold coating on the sample's surface prevents electrons from escaping the specimen. Instead of light, SEM uses electrons to form an image. Through the column of the microscope, an electron beam follows a vertical path and focuses and directs the beam down towards the sample, which makes its way through electromagnetic lenses. When an electron interacts with the sample, an incident electron beam bombards the sample's atoms. Then, the secondary electrons (SEs) and backscattered electrons (BSEs) emerge from the sample surface. The emitted electrons are collected as current, amplified, and then directed to a cathode ray tube. The electron spot and the cathode ray tube spot are swept across the specimen and tube surface to provide a picture of the sample's topography. The numerical value of magnification (M) is determined by the ratio of the length of the monitor (D) to the size of the scan on the sample (d). This is how we can see a magnified image of a sample by an SEM.

Vector Network Analyzer

In its simplest form, a VNA is an instrument used to measure impedance. It measures artificial and functional devices' S-parameters (and the corresponding number). Depending on the user interface, the size and class of these S frames are displayed in different ways. [34]. In the early 1950s, Rohde and Schwarz introduced the first instrument to measure impedance and confirm the term "network analyzer." In 1965, Wiltron introduced the 310 VNA. HP VNA followed this in 1966, 1968, and 1970. The vector network analyzer comprises three parts: a source, a receiver, and a display. When the sample was inserted into the fixture, the source applied

*Corresponding Author: **Muhammad Nasir Rafiq**

frequency (signal) to test the material and adjusted the receiver in such a way to detect the transmitted & reflected signals. To demonstrate the response of transmission and reflection measurements as a function of frequency signals, the source was transferred to the following signals, and thus, the experiment was repeated several times. When a device is put in a microwave circuit, the network vector analyzer assesses the response under test based on the scattering parameters that govern the signal flow conditions. [35]For instance, in the transmission method (S21), the E.F. of microwave signals entering the input component has been compared to signals of microwaves leaving the component. [36].

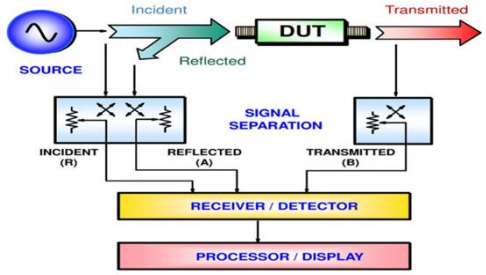

Figure 6: A Block Diagram for vector network analyzer.

Results Discussion

Phase analysis

Figure 9 displays the XRD patterns of K0.3Na0.2Bi0.5TiO3 –xBaTiO3 ceramics for phase analysis. The patterns for all studied compositions match the JCPDS card no for -------- for $K_{0.5}Bi_{0.5}TiO_3$. There appears to be a splitting of 200 peaks at 46, confirming the tetragonal phase for each ceramic composition.

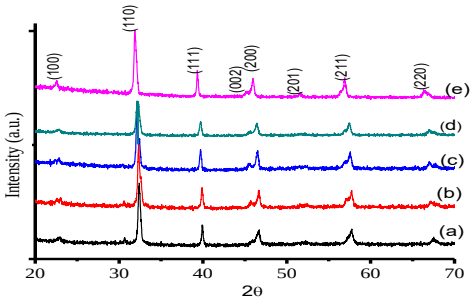

Figure. 7 Display the X-ray diffraction of (1-x) K0.3Na0.2Bi0.5TiO3 –xBaTiO3, a) x=0, b) x=0.05. c) x=0.10, d) x=0.15, e) x=0.20.

Microstructure analysis

The microstructure of the investigated ceramic in $K_{0.3}Na_{0.2}Bi_{0.5}TiO_3$ –$xBaTiO_3$ series is shown in Figure. Dense microstructure is observed for each ceramic. The average grain size for x=0 is about 1 mm, increasing with x content. Some elongated grains are also observed as the value of x rises from 0.1 to 0.20.

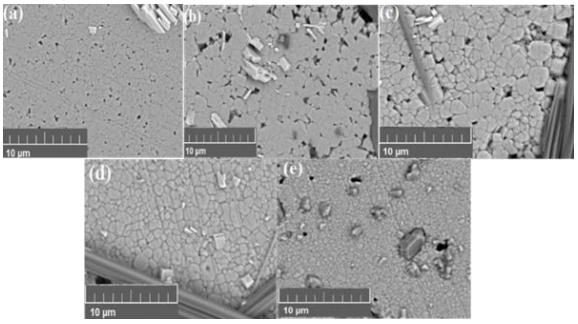

Figure. 8 Display the microstructure of (1-x) K0.3Na0.2Bi0.5TiO3 –xBaTiO3, a) x=0, b) x=0.05. c) x=0.10, d) x=0.15, e) x=0.20.

Figure: displays the piezoelectric coefficient (d_{33}) of $K_{0.3}Na_{0.2}Bi_{0.5}TiO_3$ –$xBaTiO_3$. For the composition of x=0, the d_{33} value is measured to be 90 pC/N. Previously, d33~85 has been achieved for the same composition, i.e., $K_{0.3}Na_{0.2}Bi_{0.5}TiO_3$ by Adhikary [ref].

The d_{33} value first increased from 90 to 130 pC/N with an increase in the x value from 0 to 0.10, and then it decreased to 110 with a further rise in x to 0.20. The decrease in d_{33} could be related to the rise in elongated grains in the microstructure with an increase in x >0.10.

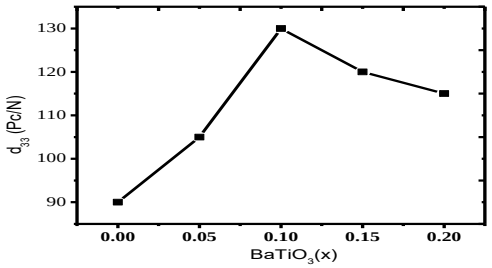

Figure9: Piezoelectric coefficient (d33) of K0.3Na0.2Bi0.5TiO3 –xBaTiO3

Figure 12 depicts the dielectric constant of the composition x=0.1 in K0.3Na0.2Bi0.5TiO3 –xBaTiO3 series. A curie temperature of about 310 C is achieved with a maximum dielectric constant of ~9000 at 1 kHz. As the frequency increased to 1 MHz, the dielectric constant decreased. The reason for the decrease in dielectric constant with an increase in frequency is that the contribution of the space change and dipolar polarisation ceased with an increase in frequency from 1 kHz to 1 MHz.

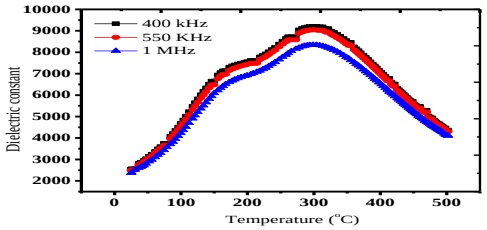

Figure. 10 Variation of dielectric constant 0.90K0.3Na0.2Bi0.5TiO3–0.1BaTiO3 with an increase in temperature at different frequencies

The figure displays the dielectric loss of $0.90K_{0.3}Na_{0.2}Bi_{0.5}TiO_3$ –$0.1BaTiO_3$ ceramics. The ceramics have a low dielectric loss from 0.1 to 0.01 in the entire temperature range from 25 ^{C}

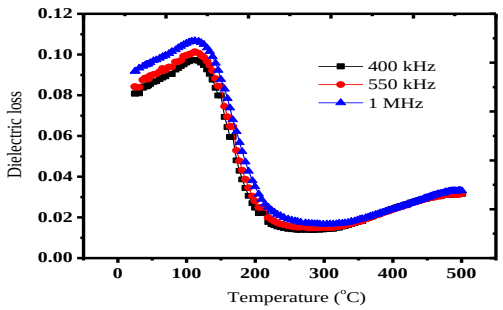

Figure. 11 Variation of dielectric constant 0.90K0.3Na0.2Bi0.5TiO3 –0.1BaTiO3 with the increase in temperature at different frequencies.

Summary and Conclusion

The BaTiO3 modified K0.3Na0.2Bi0.5 TiO3 CERAMICs were prepared using a solid-state reaction method. The XRD pattern confirms the formation of pure perovskite structure, and SEM micrographs show homogeneous microstructure with uniform particle size. The dielectric properties of the ceramic were studied as a function of frequency and temperature. The dielectric constant and dielectric loss decrease as the temperature increases. The dielectric constant, dielectric loss, ac conductivity, and dielectric permittivity were studied as a function of frequency. It was observed that the dielectric permittivity of the ceramic increases as the frequency increases. The dielectric constant and dielectric loss decrease as the frequency increases. The impedance spectra show that the impedance decreases as the frequency increases. The impedance spectra show that the impedance decreases as the frequency increases. The dielectric properties of BaTiO3-modified K0.3 Na0.2Bi0.5 TiO3 ceramics were investigated by impedance spectroscopy. The complex impedance and complex permittivity were calculated. The dielectric loss and dielectric constant were determined as a function of frequency. It was observed that the dielectric constant increases with increasing BaTiO3 content. The dielectric loss decreases as the BaTiO3 content increases. The dielectric constant and dielectric loss were lowest at the optimal BaTiO3 content of 0.5 mol%. Conversely, the dielectric constant reached its highest value at an optimal BaTiO3 content of 0.8 mol%. Additionally, the dielectric loss was also minimal at this 0.8 mol% concentration. The impedance and permittivity were at their lowest values at the optimal BaTiO3 content of 0.8 mol%, while both impedance and permittivity peaked at an optimal BaTiO3 content of 1 mol%.

References

1. Cava, R. J. (2001). Dielectric materials for applications in microwave communications Basis of a presentation given at Materials Discussion No. 3, 26–29 September 2000, University of Cambridge, UK. *Journal of Materials Chemistry*, *11*(1), 54-62.
2. Freer, R., & Azough, F. (2008). Microstructural engineering of microwave dielectric ceramics. *Journal of the European Ceramic Society*, *28*(7), 1433-1441.
3. Egerton, L., & Dillon, D. M. (1959). Piezoelectric and dielectric properties of ceramics in the system potassium—sodium niobate. Journal of the American Ceramic Society, 42(9), 438-442.
4. Fu, H., & Cohen, R. E. (2000). Polarization rotation mechanism for ultrahigh electromechanical response in single-crystal piezoelectrics. *Nature*, *403*(6767), 281-283.
5. Fu, J., Zuo, R., Fang, X., & Liu, K. (2009). Lead-free ceramics based on alkaline niobate tantalate antimonate with excellent dielectric and piezoelectric properties. *Materials Research Bulletin*, *44*(5), 1188-1190.
6. Gao, D., Kwok, K. W., Lin, D., & Chan, H. L. W. (2009). Microstructure, electrical properties of CeO2-doped (K0. 5Na0. 5) NbO3 lead-free piezoelectric ceramics. *Journal of Materials Science*, *44*(10), 2466-2470. Gao, D., Kwok, K. W., Lin, D., & Chan, H. L. W. (2009). Microstructure, electrical properties of CeO2-doped (K0. 5Na0. 5) NbO3 lead-free piezoelectric ceramics. *Journal of Materials Science*, *44*(10), 2466-2470.
7. Goldschmidt, V. M. (1929). Crystal structure and chemical constitution. *Transactions of the Faraday Society*, *25*, 253-283.
8. Gou, Q., Zhu, J., Wu, J., Li, F., Jiang, L., & Xiao, D. (2018). Microstructure and electrical properties of (1-x) K0. 5Na0. 5NbO3–xBi0. 5Na0. 5Zr0. 85Sn0. 15O3 lead-free ceramics. *Journal of Alloys and Compounds*, *730*, 311-317.
9. Greve, H., Woltermann, E., Quenzer, H. J., Wagner, B., & Quandt, E. (2010). Giant magnetoelectric coefficients in (Fe 90 Co 10) 78 Si 12 B 10-AlN thin film composites. *Applied Physics Letters*, *96*(18), 182501.
10. Groth, P. (1870). Ueber Beziehungen zwischen Krystallform und chemische Constitution bei einigen organischen Verbindungen. *Annalen der Physik*, *217*(9), 31-43.
11. Haertling, G.J.E.b.R.B.M.D., New York, *Piezoelectric and Electrooptic Ceramics. Ceramic Materials for Electronics.* 1986.
12. Hiruma, Y., Aoyagi, R., Nagata, H., & Takenaka, T. (2005). Ferroelectric and piezoelectric properties of (Bi1/2K1/2) TiO3 ceramics. *Japanese journal of applied physics*, *44*(7R), 5040.
13. Hiruma, Y., Aoyagi, R., Nagata, H., & Takenaka, T. (2004). Piezoelectric properties of BaTiO3–(Bi1/2K1/2) TiO3 ferroelectric ceramics. *Japanese journal of applied physics*, *43*(11R), 7556.
14. Hochepied, J. F., Bonville, P., & Pileni, M. P. (2000). Nonstoichiometric zinc ferrite nanocrystals: syntheses and unusual magnetic properties. *The Journal of Physical Chemistry. B*, *104(5)*, *905-912.*

*Corresponding Author: **Muhammad Nasir Rafiq**

15. Hou, Y., Zhu, M., Hou, L., Liu, J., Tang, J., Wang, H., & Yan, H. (2005). Synthesis and characterization of lead-free K0. 5Bi0. 5TiO3 ferroelectrics by sol-gel technique. Journal of crystal growth, 273(3-4), 500-503
16. Huang, T., Xiao, D., Liu, C., Li, F., Wu, B., Wu, J., & Zhu, J. (2014). Effect of SrZrO3 on phase structure and electrical properties of 0.974 (K0. 5Na0. 5) NbO3–0.026 Bi0. 5K0. 5TiO3 lead-free ceramics. *Ceramics International*, *40*(2), 2731-2735.
17. Kumar, S., Ahlawat, N., & Ahlawat, N. (2016). Microwave sintering time optimization to boost structural and electrical properties in BaTiO3 ceramics. *Journal of Integrated Science and Technology*, *4*(1), 10-16.
18. Kumari, B., R Mandal, P., & K Nath, T. (2014). Magnetic, magnetocapacitance and dielectric properties of BiFeO3 nanoceramics. *Advanced Materials Letters*, *5*(2), 84-88.
19. Kumari, K., Prasad, A., & Prasad, K. (2016). Dielectric, impedance/modulus and conductivity studies on [Bi0. 5 (Na1-xKx) 0.5] 0.94 Ba0. 06TiO3,(0.16≤ x≤ 0.20) lead-free ceramics. *Am. J. Mater. Sci*, *6*(1), 1-18.
20. Kumari, P., Rai, R., & Kholkin, A. L. (2015). Influence of BiFeTaO3 addition on the electrical properties of Na0. 4725K0. 4725Li0. 055NbO3 ceramics system using impedance spectroscopy. *Journal of Alloys and Compounds*, *637*, 203-212.
21. Kumari, P., Rai, R., Sharma, S., Shandilya, M., & Tiwari, A. (2015). State-of-the-art of lead-free ferroelectrics: A critical review. *Advanced Materials Letters*, *6*(6), 453-484.
22. Nan, C. W., Cai, N., Shi, Z., Zhai, J., Liu, G., & Lin, Y. (2005). Large magnetoelectric response in multiferroic polymer-based composites. *Physical Review B*, *71*(1), 014102.
23. Amar Nath, K., Prasad, K., Chandra, K. P., & Kulkarni, A. R. (2013). Impedance and ac conductivity studies of Ba (Pr1/2Nb1/2) O3 ceramic. *Bulletin of Materials Science*, *36*(4), 591-599.
24. Noheda, B., Cox, D. E., Shirane, G., Gonzalo, J. A., Cross, L. E., & Park, S. E. (1999). A monoclinic ferroelectric phase in the Pb (Zr 1− x Ti x) O 3 solid solution. *Applied Physics Letters*, *74*(14), 2059-2061.
25. Mhasalkar, S., W. Lee, and D.J.J.A.C.S. Readey, Processing and Characterization of BaTi 4 O 9. 1989. 72(11): p. 2154-2158.
26. Monneraye, M., Serindat, J., & JOUWERSM. C. (1968). CONTROL OF DIELECTRIC LOSSES AND TEMPERATURE COEFFICIENT OF PERMITTIVITY BY DOPING IN SOME GLASS-CERAMIC MATERIALS. *Glass Technology*, *9*(3), 70.
27. Nomura, S., Tomaya, K., & Kaneta, K. (1983). Effect of Mn doping on the dielectric properties of Ba2Ti9O20 ceramics at microwave frequency. *Japanese journal of applied physics*, *22*(7R), 1125.
28. Paladino, A.J.J.o.t.A.C.S., *Temperature-Compensated MgTi2O5-TiO2 Dielectrics.* 1971. **54**(3): p. 168-169.
29. Bijumon, P. V., & Sebastian, M. T. (2004). Temperature-stable microwave dielectric ceramics in the Ca5A2Ti1-xZrxO12 (A= Nb, Ta) system. *Journal of materials research*, *19*(10), 2922-2928.
30. Fukuda, K., Shoda, K., Kunishinge, A., Kitoh, R., & Awai, I. (1994). Microstructures in mixed phases of BaTi4O9-BaPr2Ti4O12 ceramics. *Journal of materials science letters*, *13*(17), 1290-1292.
31. Drioli, E., & Giorno, L. (2012). *Basic Aspects of Memberane Science and Engineering*. Science Press.
32. Chen, Y. C., Hong, T. H., Cheng, H. F., Chang, C. B., Leou, K. C., & Lin, I. N. (2007). Milling effect on the microwave properties of Ba2Ti9O20 investigated by EMP technique. Journal of the European Ceramic Society, 27(8-9), 3069-3073.
33. Ruska, E. (1987). The development of the electron microscope and of electron microscopy (Nobel Lecture). Angewandte Chemie International Edition in English, 26(7), 595-605.
34. Grieneisen, M. L., & Zhang, M. (2011). Nanoscience and nanotechnology: evolving definitions and growing footprint on the scientific landscape. *Small*, *7*(20), 2836-2839.
35. Teppati, V., Ferrero, A., & Sayed, M. (Eds.). (2013). *Modern RF and microwave measurement techniques*. Cambridge University Press.
36. Huang, C. L., Shen, C. H., & Lin, T. C. (2009). Dielectric properties and applications of low loss (1− x)(Mg0. 95Co0. 05) TiO3–xCa0. 8Sm0. 4/3TiO3 ceramic system at microwave frequency. *Journal of Alloys and Compounds*, *468*(1-2), 516-521.

*Corresponding Author: **Muhammad Nasir Rafiq**